THE JOURNAL OF BIOLOGICAL CHEMISTRY Vol. 280, No. 35, Issue of August 19, pp. 29885–29893, 2005

Printed in U.S.A.

Heat Shock Protein 27 Is the Major Differentially Phosphorylated Protein Involved in Renal Epithelial Cellular Stress Response and Controls Focal Adhesion Organization and Apoptosis*

Received for publication, November 10, 2004, and in revised form, May 27, 2005
Published, JBC Papers in Press, June 8, 2005, DOI 10.1074/jbc.M412708200

Marjo de Graauw‡, Ine Tijdens‡, Rainer Cramer§, Steve Corless¶, John F. Timms¶‖, and Bob van de Water‡**

From the ‡Division of Toxicology, Leiden/Amsterdam Center for Drug Research, Leiden University, 2300 RA Leiden, The Netherlands, §The BioCentre, University of Reading, Whiteknights, P. O. Box 221, Reading, Berkshire RG6 6AS United Kingdom, ¶Ludwig Institute for Cancer Research and the ‖Department of Biochemistry and Molecular Biology, University College London, Gower Street, London, WC1E 6BT, United Kingdom

We used two-dimensional difference gel electrophoresis to determine early changes in the stress-response pathways that precede focal adhesion disorganization linked to the onset of apoptosis of renal epithelial cells. Treatment of LLC-PK1 cells with the model nephrotoxicant 1,2-(dichlorovinyl)-L-cysteine (DCVC) resulted in a >1.5-fold up- and down-regulation of 14 and 9 proteins, respectively, preceding the onset of apoptosis. Proteins included those involved in metabolism, *i.e.* aconitase and pyruvate dehydrogenase, and those related to stress responses and cytoskeletal reorganization, *i.e.* cofilin, Hsp27, and α-b-crystallin. The most prominent changes were found for Hsp27, which was related to a pI shift in association with an altered phosphorylation status of serine residue 82. Although both p38 and JNK were activated by DCVC, only inhibition of p38 with SB203580 reduced Hsp27 phosphorylation, which was associated with accelerated reorganization of focal adhesions, cell detachment, and apoptosis. In contrast, inhibition of JNK with SP600125 maintained cell adhesion as well as protection against apoptosis. Active JNK co-localized at focal adhesions after DCVC treatment in a FAK-dependent manner. Inhibition of active JNK localization at focal adhesions did not prevent DCVC-induced phosphorylation of Hsp27. Overexpression of a phosphorylation-defective mutant Hsp27 acted as a dominant negative and accelerated the DCVC-induced changes in the focal adhesions as well as the onset of apoptosis. Our data fit a model whereby early p38 activation results in a rapid phosphorylation of Hsp27, a requirement for proper maintenance of cell adhesion, thus suppressing renal epithelial cell apoptosis.

Acute renal failure, caused by either ischemia/reperfusion injury or exposure to nephrotoxic xenobiotics, is still an important clinical problem. Renal proximal tubular epithelial cells (PTC)[1] are the primary target, and injury to these cells results in either the onset of necrosis or apoptosis, depending on the severity of the injury. There is increasing evidence that sublethal PTC injury results in changes in cell adhesion at the level of cellular to extracellular matrix interactions at focal adhesions (1). These interactions are under the tight control of dynamic changes of the F-actin cytoskeleton. Likewise, changes in the cellular interactions after sublethal PTC injury are generally associated with altered F-actin organization. Therefore, it is important to better understand the molecular mechanisms involved in the regulation of the F-actin cytoskeleton and impaired cell adhesion after sublethal PTC injury.

Focal adhesions are the closest contact sites between cells and the extracellular matrix. Focal adhesions are formed by a complex network of cytoskeletal, adapter, and signaling proteins. These include both structural (adapter) proteins such as paxillin, talin, vinculin, and p130 Cas, and protein-tyrosine kinases such as focal adhesion kinase (FAK), Pyk2, and Src, as well as the mitogen-activated protein kinase (MAPK) family members JNK and ERK. These proteins form a direct link between the integrin cell adhesion receptors and the F-actin network. Signaling mediated by the focal adhesion protein complex is essential in various cellular processes, including cell migration, proliferation, and survival. *In vitro* studies in freshly isolated tubules as well as primary cultured renal PTC and renal cell lines indicate an essential role of focal adhesion-mediated signaling in the molecular mechanism of PTC injury, which involves disruption of the focal adhesions and a reorganization of the F-actin network (2). Cellular stress results in activation of MAPK family members. Because these kinases also localize at focal adhesions, the possibility exists that the disturbances in cell adhesions after PTC injury are in part because of activation of these kinases. So far, such a role of MAPKs has not been studied.

The family of MAPKs consists of extracellular signal-regulated kinases (ERKs), which can be activated downstream of the growth factor receptor kinases, c-Jun N-terminal kinases (JNK), and p38 MAPK that are particularly responsive to cel-

* This work was supported in part by Netherlands Organization for Scientific Research Grants 902-21-217 and 911-02-22. The costs of publication of this article were defrayed in part by the payment of page charges. This article must therefore be hereby marked "*advertisement*" in accordance with 18 U.S.C. Section 1734 solely to indicate this fact.

** Supported by a fellowship of the Royal Netherlands Academy for Arts and Sciences. To whom correspondence should be addressed: Division of Toxicology, Leiden/Amsterdam Center for Drug Research, Leiden University, Einsteinweg 55, P. O. Box 9502, 2300 RA Leiden, The Netherlands. Tel.: 31-71-5276223; Fax: 31-71-5274277; E-mail: b.water@LACDR.LeidenUniv.nl.

[1] The abbreviations used are: PTC, proximal tubular cells; DCVC, 1,2-dichloro-vinyl-L-cysteine; 2D-DIGE, two-dimensional difference gel electrophoresis; Hsp27, heat shock protein 27; FA, focal adhesion; MALDI-TOF, matrix assisted laser desorption ionization-time-of-flight; DMEM, Dulbecco's modified Eagle's medium; c-Jun N-terminal kinase; FAK, focal adhesion kinase; MAPK, mitogen-activated protein kinase; PBS, phosphate-buffered saline; BSA, bovine serum albumin; HPLC, high pressure liquid chromatography; GFP, green fluorescent protein; CHAPS, 3-[(3-cholamidopropyl)dimethylammonio]-1-propanesulfonic acid; AMC, aminomethylcoumarin; TFEC, *S*-(1,1,2,2)-tetrafluoroethyl-L-cysteine; DPPD, *N,N*-9-diphenyl-*p*-phenylenediamine; ERKs, extracellular signal-regulated kinases; MS, mass spectrometry.

lular stress conditions such as reactive oxygen species, heat shock, and DNA damage (3). JNK and p38 have been implicated in the cellular stress signaling in the kidney after acute renal cell injury. Renal ischemia/reperfusion causes activation of JNK, p38, and ERK (4–6), possibly as a direct consequence of oxidative stress (4, 5). Also a variety of nephrotoxicants causes the activation of JNK and p38 (7–9). *In vitro* as well as *in vivo* studies using either antisense or pharmacological inhibitors suggest that sustained activation of JNK after PTC injury promotes cell death (5, 10). Moreover, sub-lethal PTC injury that results in pre-conditioning prevents the activation of JNK and p38 after an additional ischemia/reperfusion insult (11, 12); under these conditions, ERK activation was unaffected (11). Although these data indicate that JNK activation promotes cell death, the role of p38 activation in the control of PTC apoptosis is largely unknown. Moreover, the exact mechanism by which JNK and p38 affect PTC cell death is unclear. Both JNK and p38 phosphorylate various transcription factors thereby affecting gene expression and ultimately the protein expression (13–16). Alternatively, JNK and p38 (in)directly cause post-translational modification of other cellular proteins, which may also affect the biological outcome of the cellular stress response. For example, JNK can phosphorylate the anti-apoptotic protein Bcl-2, thereby sensitizing cells for apoptosis (17, 18). Alternatively, localization of JNK at focal adhesion may result in the phosphorylation of FA-associated proteins such as paxillin, thereby affecting focal adhesion turnover and cell adhesion (19). In addition, p38 MAPKs activate the MAPKAP kinase 2, which phosphorylates other downstream targets, including small heat shock proteins such as Hsp27. Hsp27 and related proteins are known to affect the actin organization as well as cell death, but their role in nephrotoxicant-induced cell death is as yet unclear.

To study PTC injury, we use 1,2-dichlorovinyl-L-cysteine (DCVC), which belongs to the group of nephrotoxic halogenated alkene *S*-cysteine conjugates (20–24). Several characteristics of DCVC make this an ideal model compound to study molecular mechanisms of nephrotoxicity. DCVC is specifically taken up by renal proximal tubular cells both *in vitro* and *in vivo* where it is bio-activated by the renal cysteine conjugate β-lyase activity, resulting in the formation of reactive intermediates that cause cell injury (23, 25). PTC injury is associated with loss of focal adhesions and cell adhesion, which is followed by caspase activation and the onset of apoptosis (20, 26, 27). Focal adhesion-mediated signaling seems to be an important component in the control of DCVC-induced apoptosis, because DCVC causes the loss of FAK phosphorylation and thereby activity and promotes the loss of focal adhesion organization (28). JNK and p38 are also activated upon DCVC treatment. This allowed us to study further the role and potential mechanism of these stress kinases in the control of cellular stress-induced loss of PTC adhesion in relation to the onset of apoptosis.

In the present study, we have used a proteomics approach using two-dimensional difference gel electrophoresis (2D-DIGE) (29–31) and mass spectrometry to identify proteins that are either alternatively expressed or post-translationally modified in a MAPK-dependent manner after DCVC-induced injury of PTC. Hsp27 was identified as the most prominent early modified protein in the cellular stress response after DCVC treatment of renal epithelial cells. This modification is related to a p38-dependent phosphorylation of Hsp27. Both p38 activity and the phosphorylation of Hsp27 are implicated in the protection of renal epithelial cells against a reorganization of focal adhesions, activation of caspases, and the onset of apoptosis caused by nephrotoxic cellular stress.

EXPERIMENTAL PROCEDURES

Materials—Dulbecco's modified Eagle's medium (DMEM), fetal calf serum, penicillin/streptomycin, PBS, and trypsin/EDTA were from Invitrogen. The Cy-3 and Cy-5 *N*-hydroxysuccinimide ester dyes were synthesized by Dr. Piers Gaffney (Ludwig Institute for Cancer Research, London, UK). SyproRuby dye was from Molecular Probes; *N,N*-9-diphenyl-*p*-phenylenediamine (DPPD) was from Aldrich; SP600125 and SB203580 were from Biomol. U0126 was from Promega. DCVC was synthesized as described (32).

Cell Culture and Treatment Conditions—The porcine renal epithelial cell line LLC-PK1 cells were maintained in DMEM supplemented with 10% (v/v) fetal calf serum and penicillin/streptomycin at 37 °C in a humidified atmosphere of 95% air and 5% carbon dioxide. pkGFP and pkGFP-FAT have been described previously (28). For preparation of stable Hsp27 expressing cell lines, LLC-PK1 cells were transfected with 0.8 μg of DNA of pcDNA3.1-Hsp27wt or pcDNA3.1-Hsp27-S19A/S82A (further referred to as Hsp27-AA) (gift from T. Takano, McGill University (33)) using Lipofectamine Plus reagent according to the manufacturer's procedures (Invitrogen). Stable transfectants were selected using 800 μg/ml G418. Individual clones were picked and maintained in complete medium containing 100 μg/ml G418. Clones were analyzed for Hsp27 expression using Western blotting and immunofluorescence. For further experiments up to five stable cell lines were used per construct. For experiments, cells were plated in either 6-cm collagen-coated dishes or on collagen-coated glass coverslips in 24-well plates and allowed to adhere overnight in complete culture medium. Cells were treated with various concentrations of DCVC for the indicated times. All incubations were performed in the presence of 20 μM DPPD (10 mM stock in dimethyl sulfoxide) to block the oxidative stress-dependent necrotic pathway but allowing for the onset of apoptosis (22, 34).

Cell Cycle Analysis—Apoptosis was determined by cell cycle analysis. Medium containing floating cells was collected. Adherent cells were washed twice with PBS, 1 mM EDTA and trypsinized. Floating cells and adherent cells that were trypsinized were pooled, centrifuged for 10 min at 2000 rpm, and resuspended in 100 μl of PBS followed by fixation in 90% ethanol (−20 °C). Fixed cells were centrifuged and washed once with PBS followed by resuspending in PBS/EDTA containing 7.5 μM propidium iodide and 10 μg/ml RNase A. After 30 min at room temperature, cells were analyzed by flow cytometry (FACSCalibur, BD Biosciences). The amount of cells in sub-G_0/G_1 was calculated using the Cellquest software (BD Biosciences).

Caspase Activity Measurement—Cells were scraped in medium and collected by centrifugation together with floating cells. The cell pellet was taken up in lysis buffer (10 mM HEPES, 40 mM β-glycerophosphate, 50 mM NaCl, 2 mM $MgCl_2$, and 5 mM EGTA) and subjected to three cycles of freezing and thawing in liquid nitrogen. The suspension was centrifuged at 13,000 rpm in a microcentrifuge for 30 min. The supernatant was collected and used to determine the protein concentration using the Bradford protein assay using IgG as a standard. Equal amounts of cell protein (10 μg) were used for measuring caspase activity using Ac-DEVD-AMC as a substrate (25 μM). AMC fluorescence was followed in time using a fluorescence plate reader (HTS 7000 Bio assay reader; PerkinElmer Life Sciences). Caspase activity was calculated as pmol/mg of cell protein/min using AMC as a standard.

Western Blot Analysis-–For Western blot analysis, cells were washed twice with PBS and lysed in ice-cold lysis buffer (50 mM HEPES, 150 mM NaCl, 1% Nonidet P-40, 1 mM EDTA, pH 7.4) plus inhibitors (2 mM 4-(2-aminoethyl)benzenesulfonyl fluoride, 100 μg/ml aprotinin, 17 μg/ml leupeptin, 1 μg/ml pepstatin, 5 μM fenvalerate, 5 μM vanadate, and 1 μM okadaic acid) for 5 min. After lysis, cells were scraped and centrifuged for 5 min at 4 °C at 14,000 rpm. Protein concentrations were determined using Coomassie protein assay reagent (Pierce). Equal amounts of protein were separated by SDS-PAGE and transferred to polyvinylidene difluoride membrane (Millipore). Blots were blocked with 5% (w/v) dry milk in TBS-T (0.15 M NaCl, 50 mM Tris-HCl, and 0.05% (v/v) Tween 20) or 5% (w/v) BSA in TBS-T overnight at 4 °C and probed with appropriate primary antibodies for 3 h at room temperature as follows: anti-cleaved caspase-3 (rabbit polyclonal, 1:1000, Pharmingen), anti-FAK (monoclonal, 1 μg/ml, BD Transduction Laboratories), anti-$Tyr(P)^{397}$-FAK (polyclonal, 0.25 mg/ml, BioSource), anti-paxillin (monoclonal, 0.5 μg/ml, BD Transduction Laboratories), anti-$Tyr(P)^{118}$-paxillin (polyclonal, 0.25 μg/ml, BioSource), anti-Hsp27 (rabbit polyclonal, 1 μg/ml, Cell Signaling), anti-$Ser(P)^{82}$-Hsp27 (rabbjt polyclonal, 1 μg/ml, Upstate Biotechnology, Inc.), anti-p38 (rabbit polyclonal, 1 μg/ml, Cell Signaling), anti-$Thr(P)^{180}$/$Tyr(P)^{182}$-p38 (rabbit polyclonal, 1 μg/ml, Cell Signaling), anti-JNK (rabbit polyclonal, 1 μg/ml, Cell Signaling), and anti-$Thr(P)^{183}$/$Tyr(P)^{185}$-JNK (rabbit polyclonal, 1 μg/ml, Promega). Thereafter blots were incubated

with horseradish peroxidase-conjugated secondary antibody (GE Healthcare) at 1:5000 dilution in TBS-T for 1 h at room temperature followed by incubation with ECL Plus reagent (Amersham Biosciences) and detection with a fluorescence imager (Typhoon 9400, Amersham Biosciences).

Preparation of Cell Extracts for 2D-DIGE—For 2D-DIGE experiments, LLC-PK1 cells were plated in 10-cm dishes (~2×10^6 cells) or 15-cm dishes (~4×10^6 cells) in complete medium and allowed to grow for 3 days. Cells were serum-starved overnight in phenol red and serum-free DMEM. Thereafter, cells were treated with the indicated concentrations of DCVC in serum/phenol red-free DMEM. Cells were lysed in DIGE lysis buffer (8 M urea, 2 M thiourea, 4% (w/v) CHAPS, and 10 mM Tris, pH 8). The extracts were syringed several times followed by a 20-min centrifugation (14,000 rpm, 4 °C). The protein concentration was determined using Coomassie protein assay reagent (Pierce). Fresh cell lysates were labeled for 30 min on ice, in the dark, with *N*-hydroxysuccinimide ester derivatives of the cyanine dyes Cy-3 and Cy-5 (4 pmol/μg protein) for DIGE analysis. Reactions were quenched with a 50-fold molar excess of lysine solution to dye for 10 min on ice. The appropriate samples were mixed and reduced with 65 mM dithiothreitol. The final volume of the samples was made up to 350 μl with DIGE lysis buffer containing 1% each of ampholines/pharmalytes (GE Healthcare) and bromphenol blue. All samples were prepared and run in triplicate.

Protein Separation by Two-dimensional Gel Electrophoresis, Gel Imaging, and Two-dimensional Blotting—For isoelectric focusing, immobilized pH gradient strips pH 3–10 (GE Healthcare) were rehydrated with the cyanine dye-labeled samples at room temperature in the dark overnight. Isoelectric focusing was performed at 20 °C using a Multiphor II electrophoresis unit (GE Healthcare). A gradient of 300–3500 V was applied over 3 h followed by a constant voltage of 3500 V for 80 kV-h. Following focusing, the immobilized pH gradient strips were equilibrated at room temperature for 15 min in equilibration buffer (6 M urea, 2% (w/v) SDS, 1% (w/v) dithiothreitol, 30% (v/v) glycerol, and 50 mM Tris, pH 6.8). The equilibrated, immobilized pH gradient strips were transferred onto 18 × 20-cm 12% uniform polyacrylamide gels for separation of proteins based on molecular weight. For DIGE analysis, gels were bonded to low fluorescent glass plates using PlusOne bind/silane solution (GE Healthcare). Each gel was run at 10 °C at a constant current of 40 mA for 5 h in Protean II gel tanks (Bio-Rad). All two-dimensional gels were scanned for Cy-3 and Cy-5 directly between low fluorescent glass plates using a 2920 2D-Master Imager at the appropriate excitation and emission wavelengths (GE Healthcare). Bonded gels were also post-stained with SyproRuby. Briefly, gels were fixed overnight in 30% methanol, 7.5% acetic acid. After washing the gels with water, total protein was detected by post-staining fixed gels with SyproRuby (Molecular Probes) for at least 3 h. Post-stained gels were washed with water to remove the excess of SyproRuby dye. Thereafter, gels were scanned using the 2920 2D Imager at the appropriate excitation and emission wavelengths (GE Healthcare). In some experiments, unlabeled two-dimensional gels were transferred onto polyvinylidene difluoride membranes overnight. Membranes were blocked with 5% BSA followed by Western blotting essentially the same as described above.

Image Analysis—All generated images were exported as .tif files for further analysis of protein and phosphorylation profiles. The 2D-DIGE images were analyzed using DeCyder software and are presented as pseudo-colored and overlaid Cy-3 and Cy-5 images prepared using Adobe Photoshop. Volumes of the spots were calculated using the differential image analysis mode of DeCyder. Matched spots from triplicate gels, which showed a statistically significant difference ($p < 0.05$) in spot volume after exposure of the cells to DCVC, had a >1.5 average fold difference in spot volume and could be detected by SyproRuby post-staining, were selected and excised from the DIGE gel using a Syprot spot picker (GE Healthcare). Spots were collected in 96-well plates and kept at −20 °C for subsequent protein identification by mass spectrometry.

Mass Spectrometry—Peptide mass mapping by MALDI-TOF MS and peptide sequencing by nano-HPLC-electrospray ionization-collision-induced dissociation MS/MS was used for analysis of gel-separated proteins (35). A standard protocol was used for in-gel proteolysis (36). MALDI-MS spectra were recorded on a Reflex III (Bruker, Coventry, UK) mass spectrometer using 2,5-dihydroxybenzoic acid as matrix and internally calibrated using tryptic autolysis peptide ion signals. Nano-HPLC-electrospray ionization-collision-induced dissociation MS/MS was performed using an Ultimate HPLC (LC Packings, Amsterdam, The Netherlands) with a PepMap C18 75-μm inner diameter (LC Packings) column at a flow rate of ~200 nl/min coupled to a Q-Tof (Micromass, Wythenshawe, UK) mass spectrometer. Spectra were processed

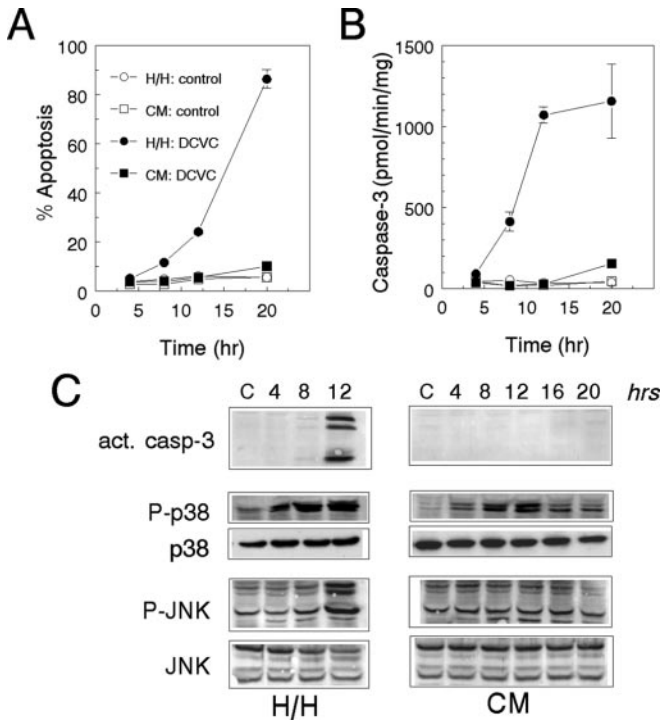

FIG. 1. **Activation of stress kinases in DCVC-induced apoptosis.** LLC-PK1 were treated with DCVC (0.25 mM) in Hanks'/HEPES (*H/H*) or complete medium (*CM*) containing 10 μM DPPD. After 4, 8, 12, and 20 h of treatment with DCVC, apoptosis was determined using cell cycle analysis (*A*), caspase-3 activity (*B*), or detection of active caspase-3 (*act. casp-3*) by Western blot analysis (*C*) as described under "Experimental Procedures." Activation of the stress kinases p38 and JNK was determined by analysis of the phosphorylation status using Western blotting (*C*). Data shown are the mean ± S.E. (*A* and *B*) and are representative of three independent experiments (*C*).

by the manufacturers' software and submitted to Mascot (37) and ProteinProspector (38) data base search routines. Peptide mass tolerance was set to 100 ppm for protein identification by peptide mass mapping. For peptide sequencing, the mass tolerance was set to 100 ppm for parent ion masses and 100 ppm or 100 millimass units for fragment ion masses. In general, significant hits from Mascot searches were considered as positive identifications. In the case of ProteinProspector searches, protein identifications were selected as significant hits by using criteria outlined in Ref. 39. A few MS/MS identifications were verified or established by manual data interpretation (*de novo* sequencing).

Immunofluorescence and Confocal Laser-scanning Microscopy—For immunofluorescence studies, cells were cultured on collagen-coated glass coverslips in 24-well dishes. Cells were fixed with 3.7% formaldehyde for 10 min followed by three washes with PBS. After cell permeabilization and blocking with PBS, 0.2% w/v Triton X-100, 0.5% w/v BSA, pH 7.4 (PTB), cells were stained for Thr(P)^{183}–Tyr(P)^{185}-JNK (Promega), Ser(P)^{82}-Hsp27 (Cellular Signaling), FAK (clone 77, BD Transduction Laboratories), Tyr(P)^{397}-FAK (BioSource), paxillin (BD Transduction Laboratories), and Tyr(P)^{118}-paxillin (BioSource) diluted in PTB. For secondary staining, Alexa488-labeled goat anti-mouse or anti-rabbit (Molecular Probes) or Cy3-labeled goat anti-mouse or anti-rabbit antibodies (Jackson Laboratories) were used. Cells were mounted on glass slides using Aqua-Poly-Mount (Polysciences Inc., Warrington, PA). Cells were viewed using a Bio-Rad 2-photon confocal laser scanning microscope, and images were processed with Adode Photoshop 6.0.

Gel Filtration Experiments—pkHsp27 and pkAA-Hsp27 cells were exposed to DCVC for 4 h and thereafter washed and lysed in 20 mM Tris, pH 7.4, 20 mM NaCl, 5 mM $MgCl_2$, 0.1 mM EDTA, and 0.1% Triton X-100. The lysates were centrifuged twice at 18,000 × *g* for 10 min, and the supernatants were applied to a Superdex 75 or a Superdex 200 10/300 GL gel filtration column (APBiotech) equilibrated in lysis buffer devoid of Triton X-100. Fractions of 1 ml were collected, and 50 μl was used for PAGE and Western blotting. Blots were stained for Hsp27. To determine accurately the sizes of the oligomeric complexes, a gel filtration standard (Bio-Rad) was used, including thyroglobulin (670 kDa),

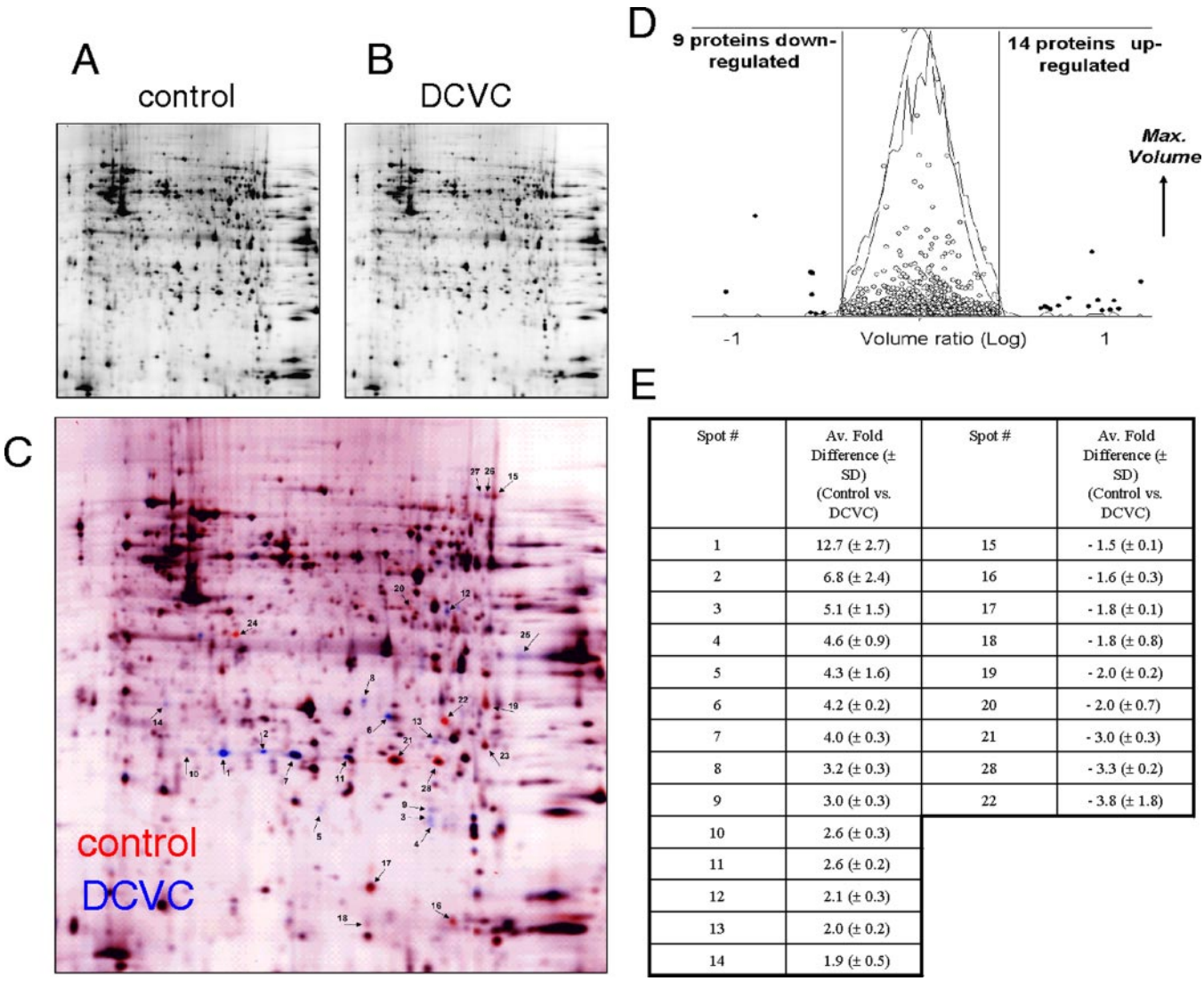

E

Spot #	Av. Fold Difference (± SD) (Control vs. DCVC)	Spot #	Av. Fold Difference (± SD) (Control vs. DCVC)
1	12.7 (± 2.7)	15	- 1.5 (± 0.1)
2	6.8 (± 2.4)	16	- 1.6 (± 0.3)
3	5.1 (± 1.5)	17	- 1.8 (± 0.1)
4	4.6 (± 0.9)	18	- 1.8 (± 0.8)
5	4.3 (± 1.6)	19	- 2.0 (± 0.2)
6	4.2 (± 0.2)	20	- 2.0 (± 0.7)
7	4.0 (± 0.3)	21	- 3.0 (± 0.3)
8	3.2 (± 0.3)	28	- 3.3 (± 0.2)
9	3.0 (± 0.3)	22	- 3.8 (± 1.8)
10	2.6 (± 0.3)		
11	2.6 (± 0.2)		
12	2.1 (± 0.3)		
13	2.0 (± 0.2)		
14	1.9 (± 0.5)		

FIG. 2. **2D-DIGE analysis of control and DCVC-treated cells.** LLC-PK1 cells were exposed to DCVC (0.25 mM) in phenol red-free DMEM for 8 h. Protein samples for 2D-DIGE were prepared and run as described under "Experimental Procedures." Control samples were labeled with Cy3 dye (*A*) and DCVC-exposed samples with Cy5 dye (*B*). The merged image (*C*) shows differences in protein expression between control (*red*) and DCVC (*blue*). Protein expression patterns were compared using DeCyder software (*D*). The >1.5 average fold differences ± S.D. were calculated for three different gels ($n = 3$) (*E*).

bovine gamma-globulin (158 kDa), chicken ovalbumin (44 kDa), equine myoglobin (17 kDa), and vitamin B_{12} (1.4 kDa).

RESULTS

Activation of Stress Kinases p38 and JNK Precedes Nephrotoxicant-induced Apoptosis of LLC-PK1 Cells—To investigate the activation of p38 and JNK in relation to chemically induced injury of renal proximal tubular epithelial cells, LLC-PK1 cells were treated with the model nephrotoxicant DCVC that causes apoptosis of renal epithelial cells in a β-lyase-dependent manner (22, 34). The induction of apoptosis (Fig. 1*A*) in association with the cleavage (Fig. 1*C*) and activation of caspase-3-like activity (Fig. 1*B*) caused by DCVC was related to an activation of JNK and p38 as determined by Western blotting using phospho-state-specific antibodies (Fig. 1*C*). For our 2D-DIGE experiment, we cultured cells in complete medium. Because amino acids present in complete medium are known to compete for uptake of DCVC and to alter the kinetics of DCVC-induced apoptosis (40), we compared the cytotoxicity of DCVC in both culture medium and our standard buffer for toxicant treatment, Hanks'/HEPES. In culture medium, DCVC-induced apoptosis was delayed and only started after 16 h of treatment (Fig. 1, *A* and *B*). Likewise, the activation of JNK and p38 was also delayed; p38 activity increased starting from 4 h, whereas JNK was barely activated (Fig. 1*C*). A slight increase in caspase-3 activity and onset of apoptosis was only evident after 20 h.

Proteomic Analysis of DCVC-induced Stress Response Using 2D-DIGE—JNK and p38 activation is associated with the phosphorylation of transcription factors such as Jun and ATF2, thereby directly affecting the expression of stress-related proteins (13). In addition, JNK and p38 can phosphorylate and thereby modulate the activity of other proteins that by themselves may also affect the cell biological outcome of a stress response. To investigate the early DCVC-induced events in more detail, we used 2D-DIGE to compare accurately the changes in the expression level and migration of proteins in total cell lysates caused by DCVC in renal epithelial cells. For proteomic analysis, we used cells that were exposed to DCVC for 8 h. To compare accurately the protein profiles, triplicate gels were made of both control and DCVC-treated LLC-PK1 cells. Lysates from control cells (labeled with Cy-3) and DCVC cells (labeled with Cy-5) were run on the same gel, and differential expression analysis was performed (Fig. 2, *A–C*). Differences in protein profiles were detected and quantitated using

TABLE I
Summary of the MS results of significantly differentially changed spots

Spot no.	Protein name	M_r	pI	ID no.	Average fold difference (±S.D.) (DCVC/ control)	Spot intensity[a] × 10^5	ID[b]
							%
1	Heat shock protein 27	22,939	6.23	P42929	12.7 (±2.7)	31.7	6:25
4	α-b-Crystallin	20,129	6.76	JC5971	4.6 (±0.9)	3.47	9:55
6	Glutathione transferase omega 1	27,491	6.36	Q9N1F5	4.2 (±0.2)	9.55	6:27
7	Heat shock protein 27	22,939	6.23	P42929	4.0 (±0.3)	53.5	6:23
8	Proteasome subunit, α-type 1	29,579	6.15	13543551	3.2 (±0.3)	4.75	10:51
10	Heat shock protein 27	22,939	6.23	P42929	2.6 (±0.3)	5.36	29:51
12	Pyruvate dehydrogenase subunit α	40,342	6.78	1917268A	2.1 (±0.3)	6.58	11:28
14	Nuclear chloride ion channel protein	26,924	5.02	AAC25675	1.9 (±0.5)	5.58	5:34
15	Aconitase hydratase	85,762	8.24	P16276	−1.5 (±0.1)	15.1	20:31
16	α-b-Crystallin	20,129	6.76	JC5971	−1.6 (±0.3)	18.1	8:43
17	Cofilin	18,519	8.16	P10668	−1.8 (±0.8)	28.1	8:57
19	Voltage-dependent anion channel	33,372	7.51	Xp032438	−2.0 (±0.2)	12.4	15:61
21	Heat shock protein 27	22,939	6.23	P42929	−3.0 (±0.3)	34.3	6:20
28	Heat shock protein 27	22,939	6.23	P42929	−3.3 (±0.2)	8.21	6:32
22	Glutathione transferase omega 1	27,491	6.36	Q9N1F5	−3.8 (±1.8)	6.42	8:32

[a] Calculated spot intensity of up-regulated proteins (Cy-5 intensity) and down-regulated proteins (Cy-3 intensity) after DCVC treatment.
[b] Number of matched peptides and their combined sequence coverage for the identified protein.

the differential in-gel analysis mode of DeCyder software and are presented as overlaid images (Fig. 2*C*; Cy-3, control shown in *red*, and Cy-5, DCVC-treated shown in *blue*). By using DeCyder, the Cy-3 and Cy-5 gel images were normalized and compared with detectable differences in spot volume (protein abundance). For each gel, DeCyder generates a histogram showing protein expression differences between control (Cy-3-labeled) and DCVC-treated (Cy-5-labeled) cells at a >1.5 average fold difference cut-off (Fig. 2*D*). Differences found on all three gels were compared, and the data were filtered to reveal significant changes in protein abundance ($p < 0.05$). At a >1.5 average fold difference cut-off, we could detect 23 differentially expressed protein spots after DCVC treatment of LLC-PK1 cells, of which nine were down-regulated (Fig. 2*E*). Gels were post-stained with SyproRuby, and all detectable changing spots were selected for identification by mass spectrometric analysis (see "Experimental Procedures"). Of the 23 differentially expressed protein spots, 15 positive identifications were obtained, representing a total of 9 different proteins (Table I), including heat shock protein 27 (Hsp27), α-b-crystallin, glutathione transferase omega 1, proteasome subunit α-type 1, pyruvate dehydrogenase, nuclear chloride ion channel protein, cofilin, aconitase hydratase, and voltage-dependent anion channel. Of the positively identified proteins, Hsp27 was the most abundant protein and was identified in several different spots. Because Hsp27 has also been linked to acute renal failure *in vivo* (11), we focused on this protein for further verification as well as its role in the mechanism of cytotoxicity.

Mobility Shift of Hsp27 after DCVC Exposure Is Related to Phosphorylation—Five different protein spots were identified as Hsp27 (Table I). To verify the identity of these spots, we performed two-dimensional Western blotting for Hsp27 using specific antibodies; all spots stained positive for Hsp27 (Fig. 3*C*). Heat shock genes, including Hsp70, are up-regulated after exposure to nephrotoxic cysteine conjugates, which is directly related to activation of heat shock factor 1 (41. 42). However, no effect of DCVC was observed on the total expression level of Hsp27 (Fig. 3*D*). In addition, other heat shock proteins, including Hsp60, Hsp70, and Hsp90, were also not yet up-regulated (data not shown). Treatment of the LLC-PK1 cells resulted in the activation of the stress kinases p38 and JNK (Fig. 1). Hsp27 is known to be phosphorylated on serine residues 15, 78, and 82 by a downstream target of p38, the MAPK-associated protein kinase (MAPKAPK)-2 (43). This suggested the possible phosphorylation of Hsp27 on these serine residues. Indeed, MS/MS peptide identification revealed the phosphorylation of the serine residue that corresponds to Ser^{82} in human Hsp27 as well as other species (Fig. 3*A*). Moreover, DCVC caused a time- and concentration-dependent Ser^{82} phosphorylation of Hsp27 as determined by one-dimensional Western blotting using a Ser^{82} phospho-specific antibody (Fig. 3*E*). DCVC-induced phospho-Ser^{82}-Hsp27 had a cytosolic localization; however, in some cells it was highly concentrated with no apparent organelle co-localization (Fig. 3*F*). This was not observed for the Hsp27 alone, suggesting a specific concentration of the phosphorylated form in these regions (data not shown). The phospho-Ser^{82}-Hsp27 was also observed on the two-dimensional Western blots; positive staining corresponded with the acidic Hsp27 spots except for the spot with the highest pI shift (Fig. 2*C, spot 1*). Despite the fact that this spot did not react strongly with both the Hsp27 and phospho-Hsp27 antibody on two-dimensional Western blots, MS/MS analysis positively identified this spot as $Ser(P)^{82}$-Hsp27 (see Table I and Fig. 3*A*). In conclusion, the data identify Hsp27 as the major early modified cellular protein after treatment with DCVC, which is related, in part, to the phosphorylation of serine residue 82.

p38 and JNK Activation Differentially Regulate Hsp27 Phosphorylation in Association with Cell Adhesion—Treatment with DCVC caused the activation of both p38 and JNK (Fig. 1). Because Hsp27 is phosphorylated on Ser^{82} by MAPKAPK-2, a target of p38, we next determined the involvement of p38 in this phosphorylation process as well as its regulation by JNK. Pharmacological inhibition of p38 with SB203580 inhibited DCVC-induced phosphorylation of Hsp27, without affecting the activity of JNK, as determined by analysis of the phosphorylation of the transcription factor c-Jun (Fig. 4*A*). Inhibition of JNK activity with SP600125 prevented the phosphorylation of c-Jun but had little effect on Hsp27 phosphorylation (Fig. 4*A*). However, SP600125 did cause a higher percentage of cells with concentrated phospho-Hsp27; moreover, under these conditions $Ser(P)^{82}$-Hsp27 co-localized in part to the F-actin network (data not shown). This was not observed in cells that were exposed to SP600125 alone. These data indicate a differential role for p38 and JNK in the control of Hsp27 phosphorylation, possibly in relation to F-actin network reorganization after stress induced by cytotoxicants. Therefore, we next wanted to determine the relative importance of these different stress kinases in the cellular response to DCVC. Nephrotoxic cysteine conjugates, including DCVC, affect the adhesion of renal epithelial cells to the extracellular matrix (20). This is associated

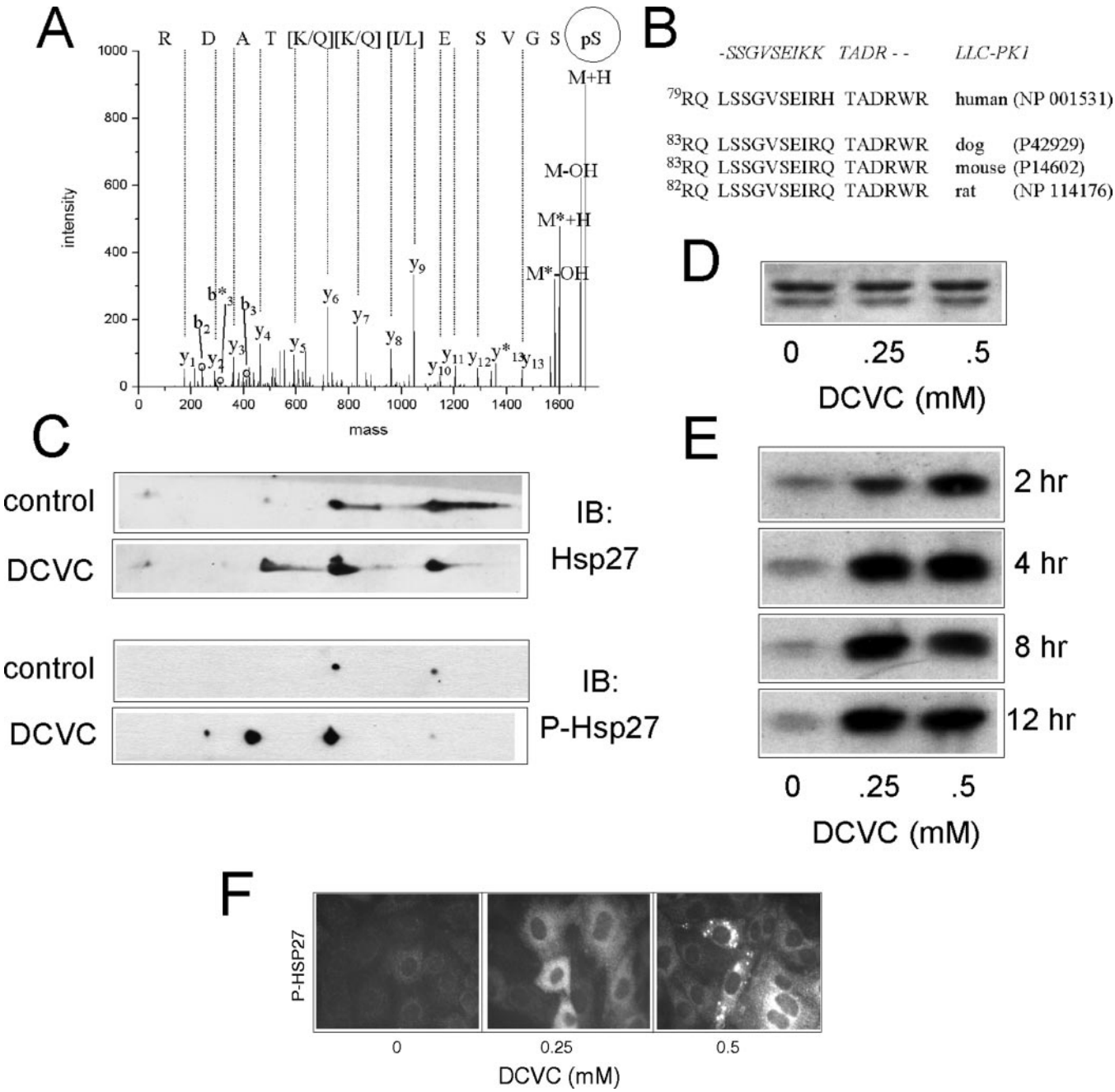

FIG. 3. **DCVC causes phosphorylation of Hsp27 on serine residue 82.** MS/MS analysis of a tryptic peptide derived from Hsp27 (*spot 1*) revealed phosphorylation on a Ser residue. *A, asterisks* indicate a loss of phosphoric acid. Alignment of the phosphopeptide pSSGVEIKKTADR with human, dog, mouse, and rat sequences (*B*). Two-dimensional Western blotting was performed as described under "Experimental Procedures" to confirm the Hsp27 mobility shift and phosphorylation on Ser^{82} after DCVC (0.25 mM) treatment. Two-dimensional blots were probed with Hsp27 and $Ser(P)^{82}$-Hsp27 antibody as described under "Experimental Procedures." *C,* LLC-PK1 cells were treated with DCVC (0.25 or 0.5 mM) in Hanks'/HEPES buffer for the indicated times, and the effects on Hsp27 expression (*D*) and phosphorylation (*E*) were analyzed by regular Western blotting. Hsp27 phosphorylation was also evaluated by immunofluorescence. *F,* data shown are representative of three independent experiments. *IB*, immunoblot.

with reorganization of the F-actin cytoskeletal network, loss of focal adhesions, and dephosphorylation of several components that are associated with focal adhesions (20, 26). Treatment of LLC-PK1 cells with DCVC alone caused a slight increase in loss of cell adhesion after 8 h (Fig. 4*B*). SB203580 caused a drastic increase of the percentage of cells that detached. In contrast, SP600125 prevented DCVC-induced cell detachment almost completely (Fig. 4*B*). Similar effects of inhibition of either p38 or JNK on DCVC-mediated changes in cell adhesion were also observed in primary cultured rat proximal tubular cells treated with DCVC (data not shown). Together, these data suggest an essential role for p38 but not JNK in the control of Hsp27 phosphorylation in association with the regulation of cell adhesion after cellular stress.

Increased Association of Activated JNK at Focal Adhesions in Association with Regulation of Focal Adhesion Turnover—Engagement between the extracellular matrix and the integrin cell adhesion receptors resulted in formation of so-called focal adhesions (FAs), the closest contact sites between cells and the extracellular matrix. FAs are large protein complexes that link the integrin receptors to the cytoskeletal network. Various cytoskeletal (regulating) proteins, adapter proteins, and signal transduction proteins are concentrated at FAs that together control a variety of cell biological processes such as cell migra-

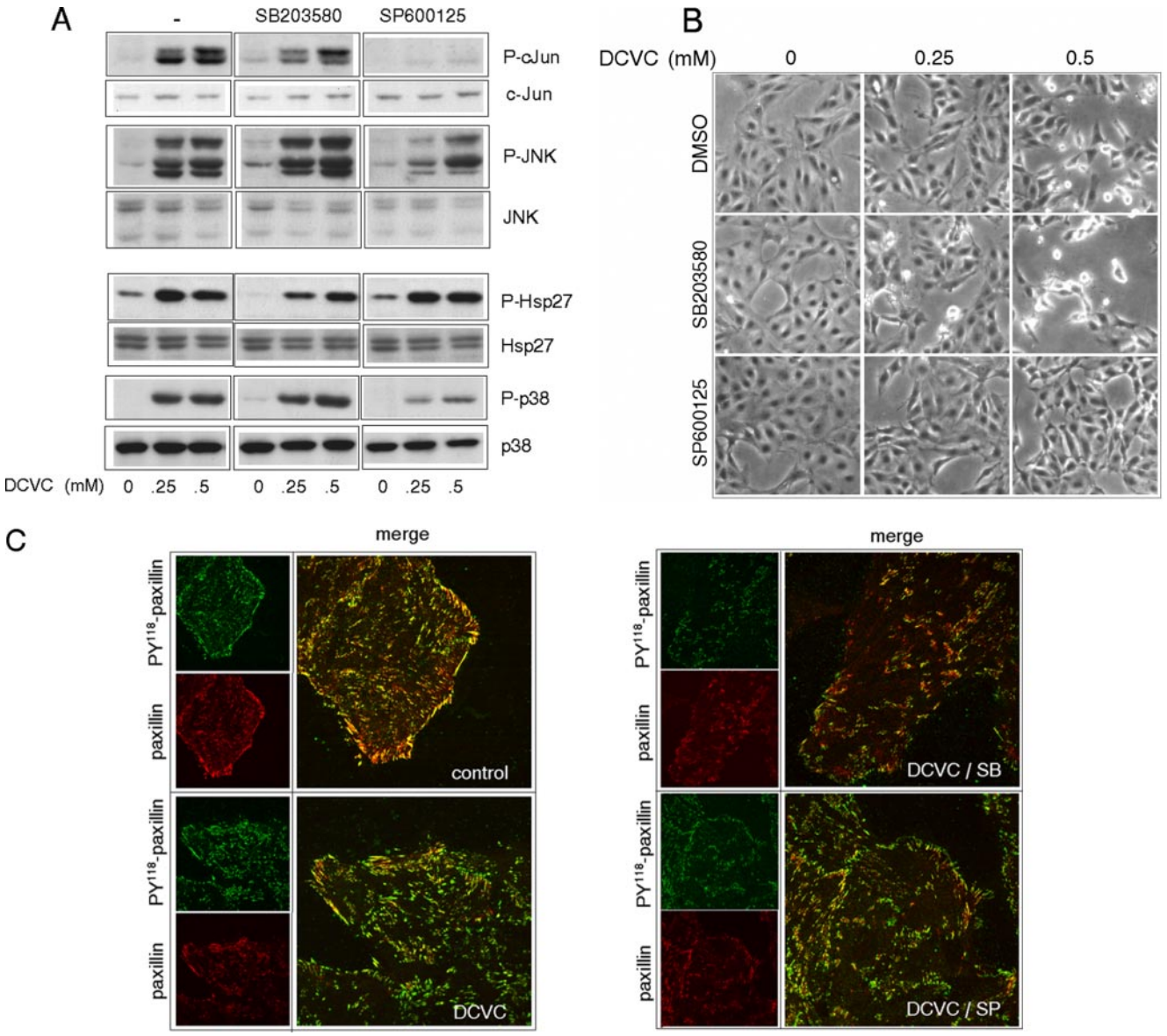

FIG. 4. **p38 and JNK regulate Hsp27 phosphorylation and cell adhesion.** LLC-PK1 cells were treated with DCVC (0.25 or 0.5 mM) in the absence or presence of the p38 inhibitor SB203580 (20 μM) or the JNK inhibitor SP600125 (20 μM) in Hanks'/HEPES buffer. After 4 h samples were taken for Western blotting to determine activation and phosphorylation of c-Jun, JNK, Hsp27, and p38. *A,* at the same time, point cell adhesion was evaluated by phase-contrast microscopy. *B,* for evaluation of focal adhesion reorganization, LLC-PK1 cells were cultured on collagen-coated coverslips, fixed, and double-stained for Tyr(P)^{118}-paxillin (*green*) and paxillin (*red*) followed by confocal laser-scanning microscopy analysis. *C,* data shown are representative of three independent experiments.

tion, proliferation, and survival. Also JNK is associated with FAs and activated upon cell adhesions (19, 44). Inhibition of Hsp27 phosphorylation with an inhibitor of p38 increased DCVC-induced cell detachment. Since under these conditions JNK activity was maintained and since inhibition of JNK prevented loss of cell adhesion, we reasoned that an increased activity of JNK at FAs is likely to be involved in the cell detachment caused by DCVC. Immunofluorescence analysis indicated not only an overall increase in levels of phosphorylated JNK after DCVC treatment, as expected based on Western blotting data (Figs. 1 and 4*A*), but also concentrated levels of phospho-JNK at sites that co-localized with the FA-associated adapter protein paxillin (Fig. 5). To rule out the possibility that the detection of phospho-JNK at FAs was related to the slight cross-reactivity of the antibody with the activated form of ERK1, cells were also treated with a selective inhibitor of MEK1, an upstream activator of ERKs. U0126 prevented ERK phosphorylation but did not affect JNK phosphorylation or the accumulation of phospho-JNK at FAs as determined by Western blotting and immunofluorescence, respectively (data not shown). Because active JNK is associated with FAs, we reasoned that JNK activity might be involved in the reorganization of FAs and oppose the action of p38. Under DCVC conditions, inhibition of JNK with SP600125 also resulted in increased association of Ser(P)^{82}-Hsp27 with punctate structures and F-actin (data not shown). Therefore, a potential role for JNK in FA turnover after cellular stress might indirectly be related to p38 activity. We determined the effect of inhibition of JNK and p38 on FA reorganization after DCVC treatment by evaluating the effect on paxillin and phosphorylated paxillin (Tyr(P)^{118}-paxillin) localization. DCVC itself caused a reorganization of FAs (*i.e.* paxillin staining) as well as F-actin structure after 4 h of treatment, which preceded the onset of apoptosis and cell detachment (Fig. 4*C*). This is in accordance with our previous findings in primary cultured rat proximal tubular cells (20). This reorganization was more prominent when cells

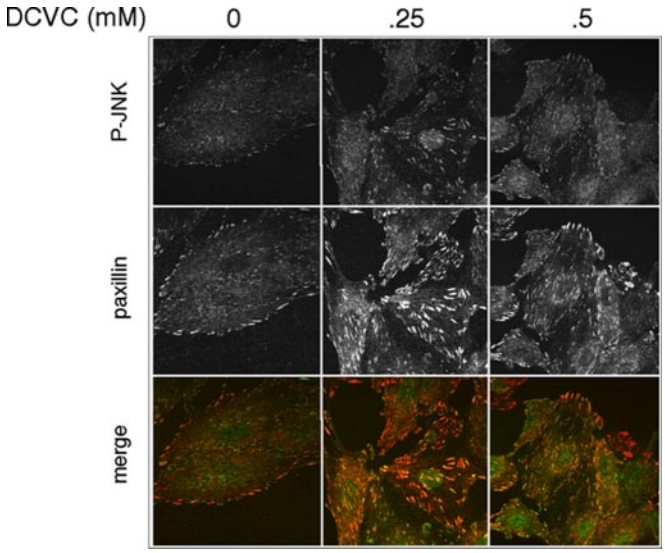

FIG. 5. **Increased localization of phospho-JNK at focal adhesions after DCVC treatment.** LLC-PK1 cells were treated with DCVC (0.25 or 0.5 mM) as described in Fig. 4. After 4 h cells were fixed and immunostained for phospho-JNK and paxillin to determine co-localization at focal adhesions. Images were generated using confocal laser-scanning microscopy. Shown is P-JNK in the *top panels*, paxillin in *middle panels*, and merge images in the *bottom panels* (P-JNK in *green* and paxillin in *red*; co-localization is *orange* to *yellow*). Data are representative of three independent experiments.

were treated with DCVC in the presence of SB203580, indicating a role of p38 in the control of focal adhesion organization; no clear effect of SP600125 on the DCVC-induced reorganization of focal adhesions was observed (Fig. 4*C*). FAK is an important player in the control of FA and its downstream signaling, which is dependent on its phosphorylation at tyrosine residue 397. Because DCVC causes the dephosphorylation of this residue prior to onset of apoptosis (20), we also evaluated a possible differential effect of SB203580 and SP600125 on FAK phosphorylation. However, no protection against FAK dephosphorylation by DCVC was observed after inhibition of either p38 or JNK (data not shown).

Recent data indicate the direct association between MEK kinase 1 and JASP1 (JNK/stress-activated protein kinase-associated protein 1) with FAK. Also, JNK can directly phosphorylate paxillin, an FA-associated adapter protein (19). Therefore, we hypothesized that FAK may be an important factor in the activation of JNK and possibly also activation of p38. To investigate this further, we used LLC-PK1 cells that overexpress a GFP-tagged dominant negative-acting deletion mutant of FAK (GFP-FAT) that lacks the N terminus. Overexpression of GFP-FAT, which competed for the localization of endogenous FAK at focal adhesion (28, 45), accelerated DCVC-induced dephosphorylation of FAK (Fig. 6*A*). DCVC caused an equal activation of both JNK and p38 in both pkGFP and pkGFP-FAT cells (Fig. 6*A*). In addition, no difference in the phosphorylation of Hsp27 and c-Jun was observed after DCVC treatment. Active phosphorylated JNK was associated with focal adhesions in pkGFP cells; however, no clear co-localization between phospho-JNK and paxillin was observed in pkGFP-FAT cells (Fig. 6*B*). After DCVC treatment, increased levels of active JNK were associated with FAs in pkGFP cells, but still no phospho-JNK associated with FAs in pkGFP-FAT cells (Fig. 6*C*). Together, these data indicate that FAK is not involved in the activation of JNK and p38 caused by DCVC, as well as the phosphorylation of Hsp27. Moreover, phospho-JNK association with FAs is not a prerequisite for c-Jun phosphorylation.

Differential Regulation of Apoptosis by p38 and JNK—Our earlier work indicated that the reorganization of FAs in association with cell detachment is important for the control of DCVC-induced apoptosis. This suggested that also inhibition of p38 by SB203580, which resulted in accelerated loss of FAs in association with cell detachment, would increase the apoptosis caused by DCVC. Inhibition of JNK with SP600125 would have the opposite effect. Indeed, SB203580 increased the percentage of apoptotic cells (Fig. 7*A*). This was associated with a higher percentage of cells that were positive for active caspase-3 as determined by immunofluorescence (Fig. 7*B*) as well as an increase in total cellular caspase-3-like activity (Fig. 7*C*). In contrast, SP600125, which prevented DCVC-induced cell detachment, also prevented the onset of apoptosis (Fig. 7). Together these data suggest a relationship between stress kinase-mediated cytoskeletal reorganization loss of FA and apoptosis.

p38-mediated Hsp27 Phosphorylation Is Associated with Protection against FA Reorganization and Apoptosis—The above findings indicate an important role for p38 and JNK in the regulation of cell adhesion and apoptosis. Because Hsp27 was identified as the most prominent early modified protein in association with p38-dependent phosphorylation, we next investigated whether Hsp27 plays a crucial role in the regulation of FAs and apoptosis after cellular stress. For this purpose we created LLC-PK1 cell lines that stably overexpress either wild type Hsp27 (pkHsp27) or mutant Hsp27 that has Ser to Ala mutations at residues 15 and 82, the two prominent MAPKAP kinase phosphorylation sites (pkAA-Hsp27). Both pkHsp27 and pkAA-Hsp27 cell lines had ~5–10-fold higher levels of Hsp27 compared with pkNeo control cell lines (Fig. 8*A*). No effect of either Hsp27 or AA-Hsp27 was observed on cell proliferation (data not shown). Next, we determined the effect of overexpression of wild type Hsp27 and AA-Hsp27 on p38 and JNK activation as well as the phosphorylation of both Hsp27 and c-Jun after treatment with DCVC. DCVC caused a similar activation of p38 in pkNeo, pkHsp27, and pkAA-Hsp27 cells. p38 activation was associated with increased levels of P-Hsp27 in pkHsp27 cells, which correlated with the increased expression of Hsp27 in these cells. No further increase in Hsp27 phosphorylation was observed in pkAA-Hsp27 cells compared with pkNeo control cells. JNK activation and c-Jun phosphorylation were comparable in all three cell lines. Next, we determined the effect on the induction of apoptosis. Overexpression of Hsp27 did not affect the percentage of apoptosis compared with Neo control cells (Fig. 8*C*). In contrast, overexpression of AA-Hsp27-sensitized LLC-PK1 cells toward DCVC induced apoptosis. To determine whether this was directly related to activation of caspases, we also determined caspase-3 like activity. Although DCVC caused activation of caspase-3-like activity in pkHsp27 cells to almost a similar extent as in pkNeo cells, a more than 2-fold increase in caspase-3 activity was observed in pkAA-Hsp27 cells. Caspase activity in untreated cells was similar in all three cell lines.

The above data indicate that activation of p38 is essential in the maintenance of focal adhesion organization after cellular stress and that p38 inhibition promotes apoptosis (Figs. 4, 5, and 7). Because Hsp27 is a downstream substrate of the p38-controlled MAPKAP kinase, we wondered whether p38-mediated Hsp27 phosphorylation controls focal adhesion organization after DCVC treatment. First, we evaluated the effect of DCVC on FAK phosphorylation. Treatment of pkNeo, pkHsp27, and pkAA-Hsp27 cells resulted in similar levels of dephosphorylation of FAK as determined by Western blotting (Fig. 8*A*). We also evaluated the organization of focal adhesions in these cells. Under normal conditions phosphorylated FAK, which specifically localizes at focal adhesions, was present at focal adhesion in the cell periphery in all three different cell

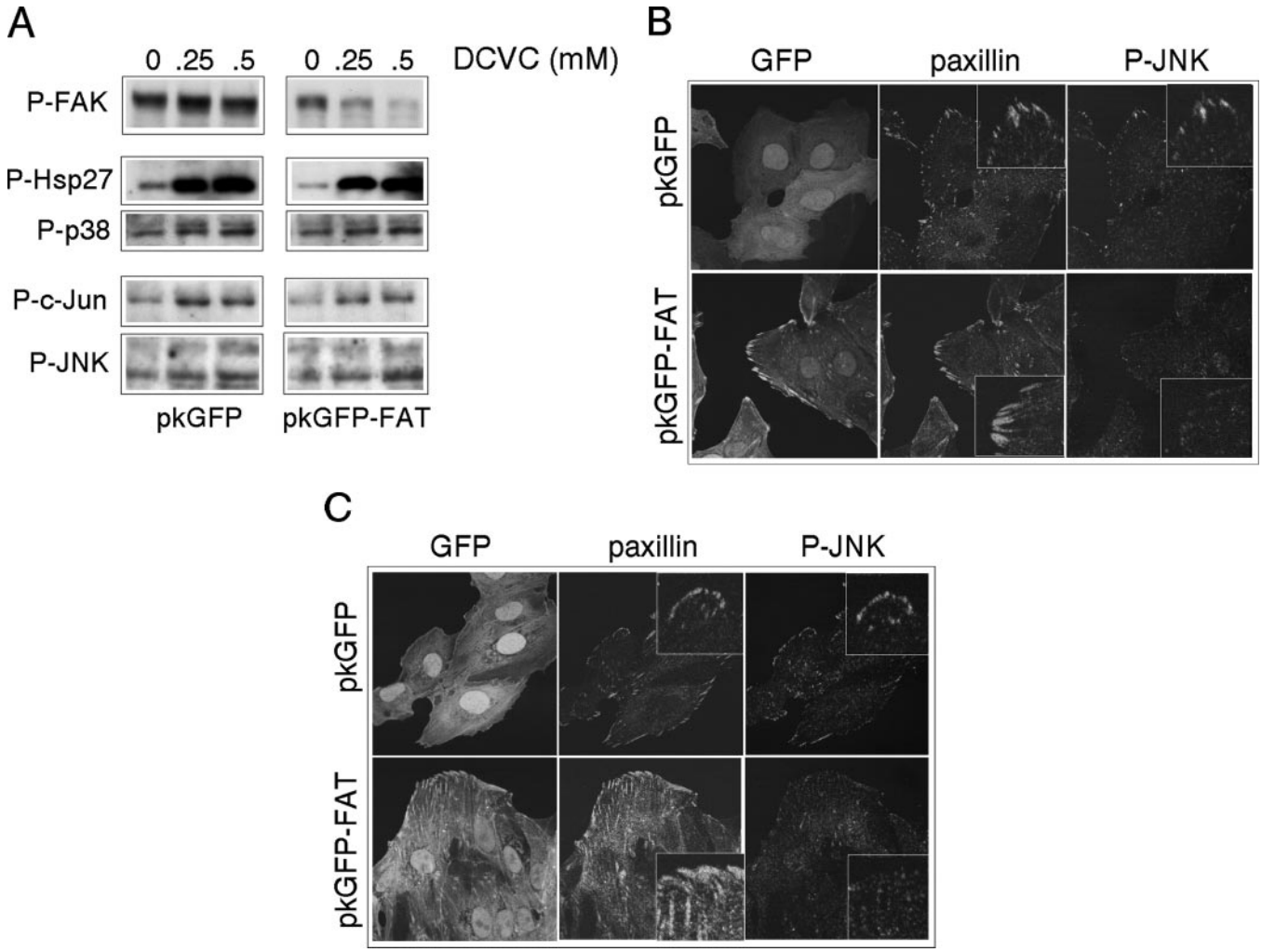

FIG. 6. **Effect of GFP-FAT overexpression on DCVC-induced activation of the stress kinases p38, JNK, and Hsp27 phosphorylation.** pkGFP and pkGFP-FAT cells were treated with DCVC (0.25 or 0.5 mM) as indicated in Fig. 4. After 4 h, samples were taken and analyzed for phosphorylation of FAK, Hsp27, p38, c-Jun, and JNK using Western blotting (*A*). Both control (*B*) and DCVC-exposed (*C*) pkGFP and pkGFP-FAT cells were fixed after 4 h followed by immunostaining for paxillin (Cy3) and P-JNK (Cy5) and analysis by confocal laser-scanning microscopy analysis of GFP, paxillin, and P-JNK. Note that *insets* in the panels of paxillin and P-JNK are enlargements of the same images. Data shown are representative for two different pkGFP and pkGFP-FAT clones observed in three different experiments.

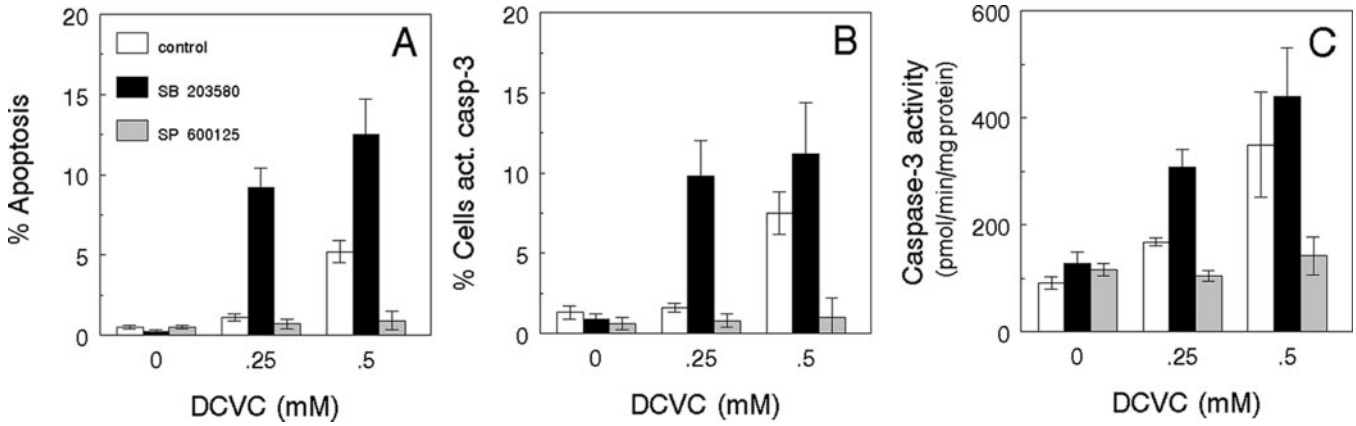

FIG. 7. **Modulation of DCVC-induced caspase 3 activation and apoptosis by p38 and JNK.** LLC-PK 1 cells were exposed to DCVC (0.25 or 0.5 mM) with or without the p38 inhibitor SB203580 (20 μM) or the JNK inhibitor SP600125 (20 μM) for 8 h as described in Fig. 4. Apoptosis was determined by counting the number of cells with a fragmented nucleus using Hoechst staining (*A*) or the percentage of cells that was positive for active caspase-3. *B,* in addition, caspase-3 activity (*C*) was determined as described under "Experimental Procedures." Data shown are the mean ± S.E. of three independent experiments ($n = 3$).

lines, whereas DCVC caused a reorganization of focal adhesions to the more central regions of the pkNeo and pkHsp27 cells; these focal adhesions were still clearly visible (Fig. 8*E*). However, in pkAA-Hsp27 cells DCVC caused a more drastic reorganization of focal adhesions; phospho-FAK localization was no longer concentrated, and paxillin localization was more

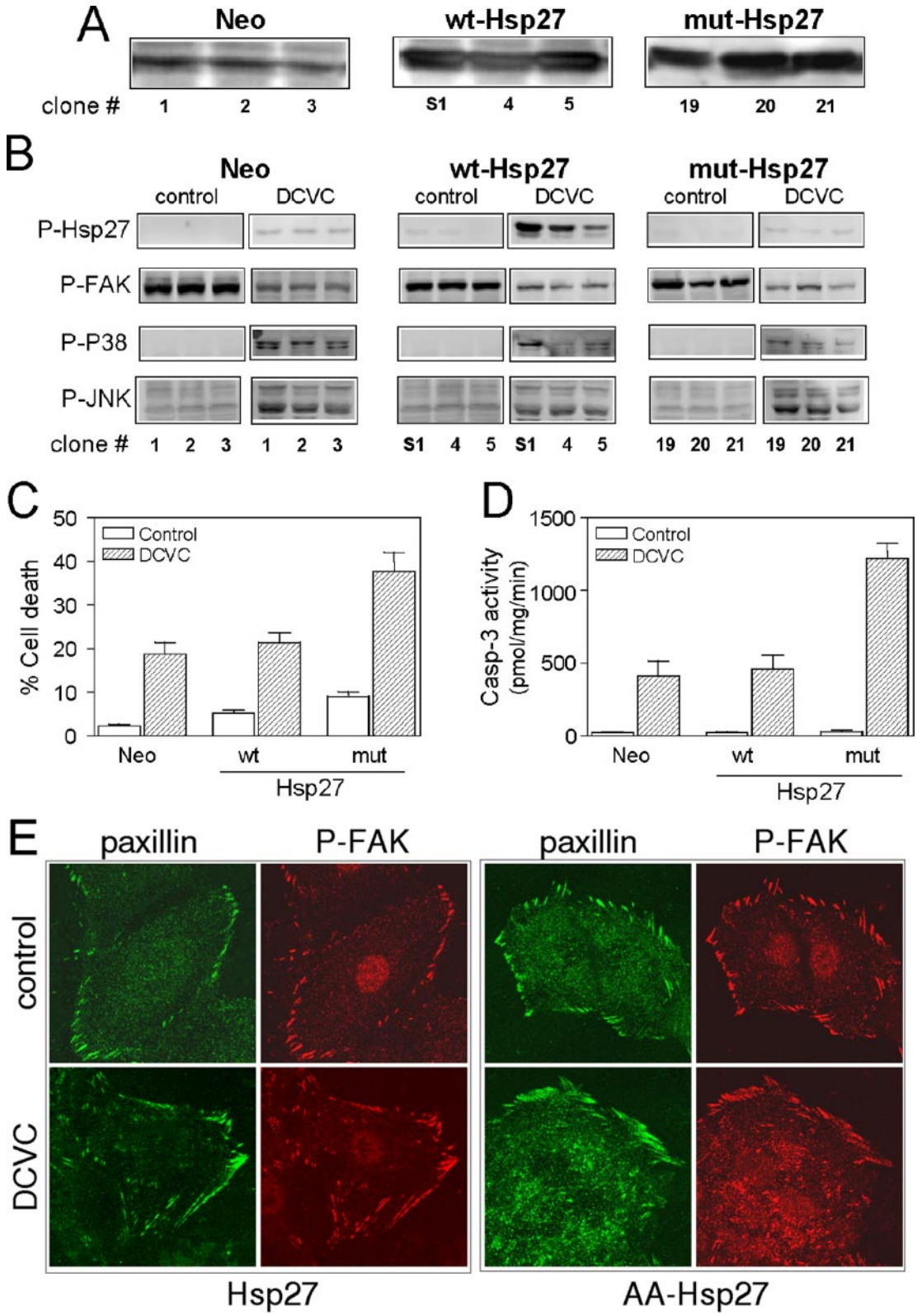

FIG. 8. **Overexpression of phosphorylation mutant Hsp27 enhances DCVC-induced apoptosis.** pkNeo, pkHsp27, and pkAA-Hsp27 were analyzed for Hsp27 expression by Western blotting as described under "Experimental Procedures." *A* and *B,* pkNeo, pkHsp27, and pkAA-Hsp27 were exposed to DCVC (0.25 mM) as described in Fig. 4, and after 8 h samples were taken and analyzed for phosphorylation of Hsp27, FAK, p38, and JNK using Western blotting. *B,* 12 h after treatment, the percentage apoptosis was determined by using cell cycle analysis (*C*), and caspase-3 activity was determined by measuring DEVDase activity (*D*) as described under "Experimental Procedures." Data shown are the mean ± S.D. of three (pkNeo) or five (pkHsp27 and pkAA-Hsp27) independent clones (n = 3–5). Data are representative of two independent experiments. *E,* to determine the effect of pkAA-Hsp27 on focal adhesion reorganization after DCVC treatment, cells were fixed and immunostained for paxillin (*green*) and Tyr(P)^{397}-FAK (*red*) followed by confocal laser-scanning microscopy analysis. Images shown are from pkHsp27 (clone 4) and pkAA-Hsp27 (clone 20) and are representative for the effects observed in the other pkHsp27 and pkAA-Hsp27 clones in two independent experiments.

distributed over the entire cell (Fig. 8*E*). Together, these data indicate an essential role for Hsp27 phosphorylation in the control of cellular stress-induced apoptosis in renal epithelial cells in close association with maintenance of cellular-extracellular matrix adhesion complexes.

Oligomeric Organization of Hsp27 Is Not Affected in pkAA-Hsp27 Cells—Small heat shock proteins (small Hsp, including Hsp27) can form oligomeric complexes with molecular complexes ranging from around 100 to 800 kDa. Phosphorylation of small heat shock proteins may lead to changes in the oligomeric organization resulting in smaller oligomers, which are responsible for stabilization of the actin filaments, and larger oligomers, which may act as chaperones thereby protecting against cellular stress (46–48). To study the influence of DCVC-induced changes in Hsp27 phosphorylation on oligomeric organization of Hsp27, we analyzed pkHsp27 and pkAA-Hsp27 cells treated with DCVC for oligomeric sizes by size exclusion gel filtration using either Superdex 75 or Superdex 200 columns. Our analysis shows that Hsp27 is present as large oligomers (800–600 kDa) as well as small oligomers (200–100 kDa) and monomers (27 kDa) in both cell lines either treated or untreated (Fig. 9*A*). In pkHsp27 cells, DCVC caused a slight shift in the levels of around 800–600 kDa (fractions 11 and 12) toward the 200–100-kDa (fractions 14 and 15) complexes; no increase in monomeric Hsp27 (fractions 19 and 20) was observed. In pkAA-Hsp27 cells this DCVC-induced shift did not occur. To calculate more precisely the relative amount of monomeric Hsp27 compared with the oligomeric forms of Hsp27, we used a Superdex 75 column. With this column we were able to obtain more concentrated fractions; all the monomeric Hsp27 proteins were eluted in one single fraction (fraction 10), whereas all the oligomeric forms were eluted in fractions 8 and 9. For both control as well as DCVC-treated cells, we observed ~40% of Hsp27 protein in the oligomeric fractions (*lanes 8* and *9*) and 30% in the fraction containing monomer Hsp27 (*lane 8,* Fig. 9*B*). No difference was observed between pkHsp27 or pkAA-Hsp27 cells, further supporting our findings of the Superdex 200 column that no major shift occurred in the levels of monomeric Hsp27. It would be relevant to determine in which fraction the phosphorylated form of Hsp27 is present, which of course can only be observed in the pkHsp27 and not the pkAA-Hsp27 cells. Unfortunately, it was not possible to detect phosphorylated Hsp27 in the samples most likely because of the dilution of the samples of the cell lysate after size exclusion chromatography and/or limited sensitivity of the Ser(P)^{82}-Hsp27 antibody staining. These data suggest that subtle changes in the size of oligomeric complexes rather than the levels of monomeric Hsp27 may determine the differences between pkHsp27 and pkAA-Hsp27 cells with respect to DCVC-induced cytotoxicity.

DISCUSSION

In the present study we have used 2D-DIGE and mass spectrometry to identify proteins that are differentially expressed and/or post-translationally modified prior to the onset of renal proximal tubular cell apoptosis caused by the nephrotoxic cysteine conjugate DCVC. By using this and other approaches, we were able do the following: 1) to identify nine different proteins that play a role in the regulation of the actin cytoskeletal network, cellular metabolism, and cellular stress responses; 2) to define that Hsp27 is a protein that is affected most after DCVC-induced renal cell injury (Hsp27 changes are related to increased phosphorylation of Hsp27 in a p38-dependent manner); and 3) to determine the importance of Hsp27 phosphorylation in suppression of the onset of renal cell apoptosis. These effects of Hsp27 appear to be related to control of focal adhesion turnover.

As mentioned, we were able to identify proteins that may play a role in DCVC-induced cytotoxicity. It should be stressed, however, that the conditions we used for our proteomics approach were mild; cells were treated with DCVC in culture medium, which resulted in the onset of cytotoxicity only after 24 h. The reduced cytotoxicity of DCVC under these conditions is most likely because of the reduced uptake of DCVC by cysteine carriers due to the presence of L-cysteine in the medium. Although our findings may therefore not reflect typical exposure conditions for DCVC to determine the mechanism of toxicity, the identified proteins are most likely the first proteins that are modified and therefore crucial in the early phases of cellular injury caused by DCVC. Two of the proteins that we identified are involved in cellular metabolism, aconitase hydratase and the α subunit of pyruvate dehydrogenase. Aconitase, which is located in the mitochondrial matrix, was recently identified as a direct target for covalent modification by a structural and mechanistically similar nephrotoxic cysteine conjugate, *S*-(1,1,2,2)-tetrafluoroethyl-L-cysteine (TFEC), which is also metabolized by renal proximal tubular cells in a β-lyase-dependent manner resulting in the formation of a thioalkylating reactive intermediate. In fact, aconitase seems part of a functional multienzyme complex that also contains other proteins that are directly modified by TFEC, including two subunits of α-ketoglutarate-dehydrogenase, lipoamide succinyltransferase and dihydrolipoamide dehydrogenase. In the 2D-DIGE experiments, aconitase was present in two protein spots with identical molecular weights but with different pI values as determined by two-dimensional Western blotting with aconitase antibodies (data not shown). DCVC caused the formation of two additional acidic aconitase spots and a decrease in the level of the most prominent basic aconitase spot. These differences in the pI values of aconitase are possibly due to the modification of the labile 4Fe-4S clusters in aconitase that are required in the dehydration-rehydration of citrate to isocitrate in the Krebs cycle. Likewise, modification of aconitase by cysteine conjugates may affect these Fe-S clusters and, thereby, the pI characteristics of the protein and possibly the enzyme activity. Indeed, modification of aconitase by TFEC causes an inhibition of aconitase enzyme activity (49). Although we do not know the exact reason for the changes in protein spots in our two-dimensional gels (*i.e.* direct covalent modification, altered transcription/translation, or phosphorylation), the identified proteins fit with the current understanding that nephrotoxic cysteine conjugates directly affect mitochondrial function.

We also identified several proteins that are important in the control of the actin cytoskeletal network, including cofilin, Hsp27, and α-b-crystallin. This supports our previous finding that DCVC causes drastic changes in the organization of the F-actin network (22). These changes may well be related to alterations in the expression and/or activity of cofilin. Also Hsp27 and α-b-crystallin have been associated with the regulation of F-actin network organization, although this has not been shown for renal epithelial cells.

The most prominent changes after cellular stress in LLC-PK1 cells were observed in Hsp27, which belongs to the family of small heat shock proteins that also includes α-B-crystallin. No difference in the total cellular level of Hsp27 was observed after DCVC treatment. Instead, changes in the two-dimensional protein profile of Hsp27 were primarily due to increased phosphorylation of Hsp27, which explained a pI shift to the acidic region. By using mass spectrometry, we identified phosphorylation of Hsp27 on Ser^{82}. Although phosphorylation of this residue was verified by both Western blotting and immunofluorescence using phospho-state-specific antibodies against this phosphorylated residue, it did not fully explain the multi-

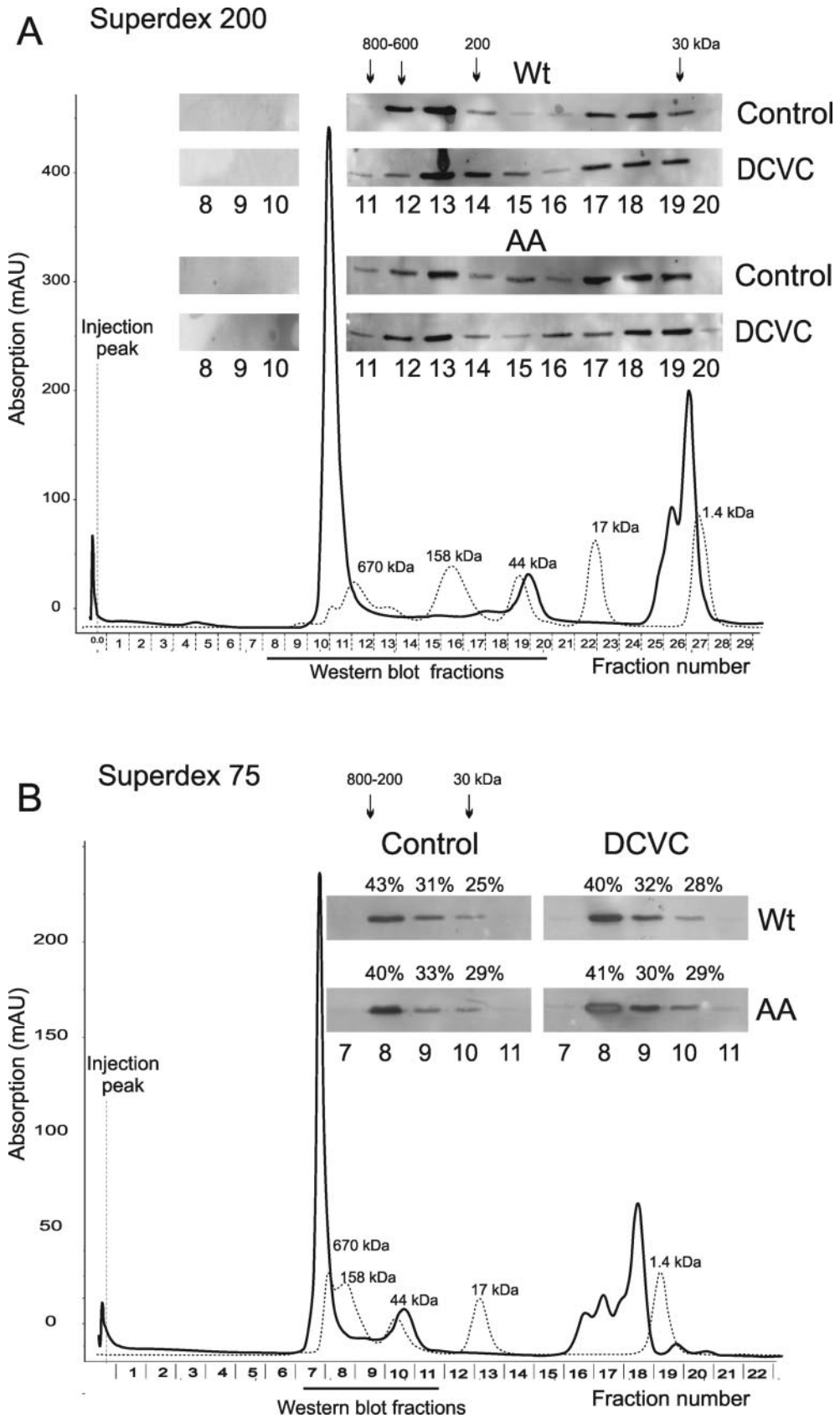

FIG. 9. **Effect of DCVC on Hsp27 oligomerization in pkHsp27 and pkAA-Hsp27 cells.** pkHsp27 and pkAA-Hsp27 were exposed to 0.25 mM DCVC for 4 h, and cell lysates were prepared as described under "Experimental Procedures." The degree of oligomerization was determined using size exclusion gel filtration on a Superdex 200 (*A*) or Superdex 75 column (*B*) (AP Biotech), both calibrated with a gel filtration standard (Bio-Rad), including the marker proteins thyroglobulin (670 kDa), bovine gamma-globulin (158 kDa), chicken ovalbumin (44 kDa), equine myoglobin (17 kDa), and vitamin B_{12} (1.4 kDa). 50 μl of total cell lysate (0.2 mg of protein) was applied to each column, and fractions of 1 ml were collected. The *solid line* shows the relative absorbance (280 nm) of proteins in the total cell lysate, and the *dashed line* shows the 280 nm chromatogram of all marker proteins. The presence of Hsp27 in the fractions eluted of the column was detected by immunoblotting (50 μl per lane for each fraction) using an Hsp27 antibody (*insets*). The *arrows* indicate which fractions contain Hsp27 oligomers and monomers.

ple Hsp27 spots that were identified by 2D-DIGE. Hsp27 is also phosphorylated on Ser^{15} and Ser^{78} in LLC-PK1 cells, which could account for the additional spots observed in the two-dimensional Western blots. Regardless of the exact modification of Hsp27 by phosphorylation, stable overexpression in LLC-PK1 cells of a $Ser^{15} \rightarrow Ala/Ser^{82} \rightarrow Ala$-Hsp27 mutant accelerated the onset of apoptosis caused by DCVC, underscoring the role of these two Hsp27 modifications in the control of renal cell death. Although adenovirus-mediated overexpression of wild type Hsp27 also inhibits cell death of LLC-PK1 cells caused by either oxidative stress or ATP depletion (12), in our hands overexpression of wild type Hsp27 itself did not provide cytoprotection. Most likely the phosphorylation of endogenous Hsp27 is already sufficient to provide protection, and the phosphorylation-defective mutant Hsp27 acts as a dominant negative for the function of endogenous Hsp27. Alternatively, adenovirus-mediated transduction of Hsp27 results in far higher levels of Hsp27 than in our stable transfected cell lines.

Because phosphorylation of Hsp27 may influence the oligomeric organization of Hsp27, thereby affecting its stress-protective chaperone function, we determined the effect of inhibition of Hsp27 phosphorylation on the formation of oligomeric complexes (50, 51). Replacement of Ser^{15} and Ser^{82} by Ala slightly affected the size of large oligomers of Hsp27 in DCVC-treated cells (Fig. 9*A*); however, no change in the levels of monomeric Hsp27 was observed. Mehlen *et al.* (46) showed that a triple Ser mutant leads to the formation of large aggregates compared with wild type Hsp27, whereas only a triple and not a mono- or double phospho-mimicking mutant resulted in a significant decrease in large oligomers (47). We used a double mutant in our studies that already sensitized cells for the onset of apoptosis. Because phosphorylation of Hsp27 is very rapid and transient, newly formed oligomers are rapidly created thereby enhancing the chaperone function of Hsp27. The differences in apoptotic cell death between pkHsp27 and pkAA-Hsp27 cells may well be due to a slower turnover of large oligomers in mutant cells resulting in higher levels of unfolded proteins, which is supported by our data in Fig. 9*A*. In addition, phosphorylated, monomeric forms of Hsp27 may protect cells against apoptosis by stabilizing the cytoskeletal network (48). Although the amounts of Hsp27 monomers did not differ between pkHsp27 and pkAA-Hsp27 cells (Fig. 9*B*), the phosphorylation status does differ. The unphosphorylated Hsp27 in the pkAA-Hsp27 cells is not capable of F-actin stabilization and protection of focal adhesion reorganization resulting in enhanced apoptotic cell death.

Phosphorylation of Hsp27 on Ser^{82} is mediated by MAPKAP kinase 2, which is activated by p38. In our hands, the Ser^{82} phosphorylation of Hsp27 was dependent on p38 activity because SB203580 inhibited it, although some phosphorylated Hsp27 could still be observed. This remaining phosphorylation of Hsp27 might be due to MAPKAP kinase 2 activation occurring independent of p38. Indeed, SB203580 does not completely prevent stress-induced activation of MAPKAP-2 in LLC-PK1 cells (8). Alternatively, other protein kinases activated because of DCVC treatment could potentially phosphorylate Hsp27 (8). This may also explain the effect observed by inhibition of JNK with SP600125, which resulted in decreased levels of phosphorylated p38 levels without affecting the stress-induced phosphorylation of Hsp27 (Fig. 4*A*). Under the latter circumstances, the observed effects may also be a reflection of changes in the dynamics of p38 activation *versus* Hsp27 phosphorylation and/or dephosphorylation. The exact mechanism and the involvement of different protein kinases and phosphatases requires further investigation. Inhibition of p38 itself with SB203580 did not affect p38 phosphorylation, which is most likely due to the fact that the phosphorylation is mediated by protein kinases (*i.e.* MMK3/6) that are not affected by SB203580.

Inhibition of p38 with SB203580 accelerated the reorganization of focal adhesions after DCVC treatment; this was associated with a more rapid cell detachment and onset of apoptosis. In a similar fashion, stable overexpression of the Hsp27 phosphorylation mutant in LLC-PK1 cells also increased the susceptibility toward reorganization of focal adhesions caused by DCVC as well as the induction of apoptosis. Together these data fit with a model whereby cellular stress causes activation of p38 thereby resulting (indirectly) in phosphorylation of Hsp27, which in turn protects against the cellular insult. Although our data support a role for Hsp27 phosphorylation in protection against the reorganization of focal adhesions, overexpression of mutant Hsp27 does not protect against a dephosphorylation of FAK. So far, we do not know the exact mechanism by which Hsp27 affects focal adhesion organization. Moreover, it cannot be excluded that Hsp27 phosphorylation also modulates other routes that are essential for the onset of apoptosis. Recent studies indicate that Hsp27 suppresses apoptosis by maintenance of the F-actin network organization, thereby preventing the mitochondrial release of cytochrome *c* (52). F-actin disruption as a result of cell injury causes the release of the Bcr homology 3-only pro-apoptotic Bcl-2 family member Bmf that activates the mitochondrial pathway of apoptosis (53); such a release is likely to be prevented if Hsp27 preserves F-actin organization. Alternatively, Hsp27 can bind cytochrome *c*, which is an essential component for the formation of the apoptosome and activation of caspase-9 and ultimately caspase-3 (54).

DCVC also caused the activation of JNK, which was associated with focal adhesions. Inhibition of JNK with SP600125 inhibited cell detachment and apoptosis. JNK localization at focal adhesions is mediated through FAK (44). Overexpression of GFP-FAT in LLC-PK1 cells prevents the localization of FAK at focal adhesions, although there was an accelerated FAK dephosphorylation after DCVC treatment. In GFP-FAT cells little active JNK was associated with focal adhesions. Nevertheless, in GFP-FAT cells DCVC caused an equal c-Jun phosphorylation as well as a p38-mediated Hsp27 phosphorylation, thus excluding a role for localization of active JNK is these stress responses. Although inhibition of JNK inhibited cell detachment, no clear protection against DCVC-induced focal adhesion reorganization was observed. Also, inhibition of JNK did not affect focal adhesion reorganization in either DCVC-treated pkHsp27 or pkAA-Hsp27 cells (data not shown). In contrast, SP600125 improved the maintenance of adherens junctions as determined by immunofluorescence staining for β-catenin (data not shown). Paxillin, a downstream substrate of the FAK/Src kinase complex at focal adhesions, is a downstream substrate of JNK, which seems related to the turnover of focal adhesions. In LLC-PK1 cells, some paxillin is seen at cell-cell junctions. Therefore, it is possible that JNK will phosphorylate paxillin at these cell-cell adhesion sites thereby inducing a loss of cell-cell adhesions. Alternatively, other yet to be identified substrates of JNK may affect these adhesions. Although our data suggest a relationship between JNK-dependent loss of cell adhesion and the onset of apoptosis, we cannot exclude that DCVC-induced JNK activation results in the phosphorylation of other cellular proteins that (in)directly affect the onset of apoptosis.

Altogether, our 2D-DIGE approach resulted in the identification of proteins that have been identified previously either as direct targets of nephrotoxic cysteine conjugates or as proteins being up-regulated after renal toxic stress. Hsp27 phosphoryl-

ation plays a role in the suppression of the onset of cell death in renal cells. Future studies are required to evaluate the role of the other modified proteins in the control of nephrotoxicity.

Acknowledgments—We thank Dr. Takano for Hsp27 constructs, Dr. Marcellus Ubbink and Drs. Thyra de Jongh for assistance with gel filtration experiments, and members of the division of Toxicology of the Leiden/Amsterdam Center for Drug Research for valuable discussion and support.

REFERENCES

1. Molitoris, B. A., and Marrs, J. (1999) *Am. J. Med.* **106,** 583–592
2. Weinberg, J. M., Venkatachalam, M. A., Roeser, N. F., Senter, R. A., and Nissim, I. (2001) *Am. J. Pathol.* **158,** 2153–2164
3. Johnson, G. L., and Lapadat, R. (2002) *Science* **298,** 1911–1912
4. DiMari, J., Megyesi, J., Udvarhelyi, N., Price, P., Davis, R., and Safirstein, R. (1997) *Am. J. Physiol.* **272,** F292–F298
5. Kunduzova, O. R., Bianchi, P., Pizzinat, N., Escourrou, G., Seguelas, M. H., Parini, A., and Cambon, C. (2002) *FASEB J.* **16,** 1129–1131
6. Pombo, C. M., Bonventre, J. V., Avruch, J., Woodgett, J. R., Kyriakis, J. M., and Force, T. (1994) *J. Biol. Chem.* **269,** 26546–26551
7. Hayakawa, J., Depatie, C., Ohmichi, M., and Mercola, D. (2003) *J. Biol. Chem.* **278,** 20582–20592
8. Dong, J., Ramachandiran, S., Tikoo, K., Jia, Z., Lau, S. S., and Monks, T. J. (2004) *Am. J. Physiol.* **287,** F1049–F1058
9. Yuan, Z. Q., Feldman, R. I., Sussman, G. E., Coppola, D., Nicosia, S. V., and Cheng, J. Q. (2003) *J. Biol. Chem.* **278,** 23432–23440
10. Garay, M., Gaarde, W., Monia, B. P., Nero, P., and Cioffi, C. L. (2000) *Biochem. Pharmacol.* **59,** 1033–1043
11. Park, K. M., Chen, A., and Bonventre, J. V. (2001) *J. Biol. Chem.* **276,** 11870–11876
12. Park, K. M., Kramers, C., Vayssier-Taussat, M., Chen, A., and Bonventre, J. V. (2002) *J. Biol. Chem.* **277,** 2040–2049
13. Gupta, S., Barrett, T., Whitmarsh, A. J., Cavanagh, J., Sluss, H. K., Derijard, B., and Davis, R. J. (1996) *EMBO J.* **15,** 2760–2770
14. Tan, Y., Rouse, J., Zhang, A., Cariati, S., Cohen, P., and Comb, M. J. (1996) *EMBO J.* **15,** 4629–4642
15. Pulverer, B. J., Kyriakis, J. M., Avruch, J., Nikolakaki, E., and Woodgett, J. R. (1991) *Nature* **353,** 670–674
16. Hazzalin, C. A., Cano, E., Cuenda, A., Barratt, M. J., Cohen, P., and Mahadevan, L. C. (1996) *Curr. Biol.* **6,** 1028–1031
17. Deng, X., Xiao, L., Lang, W., Gao, F., Ruvolo, P., and May, W. S., Jr. (2001) *J. Biol. Chem.* **276,** 23681–23688
18. Yamamoto, K., Ichijo, H., and Korsmeyer, S. J. (1999) *Mol. Cell. Biol.* **19,** 8469–8478
19. Huang, C., Rajfur, Z., Borchers, C., Schaller, M. D., and Jacobson, K. (2003) *Nature* **424,** 219–223
20. van de Water B., Nagelkerke, J. F., and Stevens, J. L. (1999) *J. Biol. Chem.* **274,** 13328–13337
21. van de Water B., Jaspers, J. J., Maasdam, D. H., Mulder, G. J., and Nagelkerke, J. F. (1994) *Am. J. Physiol.* **267,** F888–F899
22. van de Water B., Kruidering, M., and Nagelkerke, J. F. (1996) *Am. J. Physiol.* **270,** F593–F603
23. Chen, J. C., Stevens, J. L., Trifillis, A. L., and Jones, T. W. (1990) *Toxicol. Appl. Pharmacol.* **103,** 463–473
24. Zhang, G. H., and Stevens, J. L. (1989) *Toxicol. Appl. Pharmacol.* **100,** 51–61
25. Stevens, J. L., Robbins, J. D., and Byrd, R. A. (1986) *J. Biol. Chem.* **261,** 15529–15537
26. Gailit, J., Colflesh, D., Rabiner, I., Simone, J., and Goligorsky, M. S. (1993) *Am. J. Physiol.* **264,** F149–F157
27. Goligorsky, M. S., Lieberthal, W., Racusen, L., and Simon, E. E. (1993) *Am. J. Physiol.* **264,** F1–F8
28. van de Water, B., Houtepen, F., Huigsloot, M., and Tijdens, I. B. (2001) *J. Biol. Chem.* **276,** 36183–36193
29. Unlu, M., Morgan, M. E., and Minden, J. S. (1997) *Electrophoresis* **18,** 2071–2077
30. Gharbi, S., Gaffney, P., Yang, A., Zvelebil, M. J., Cramer, R., Waterfield, M. D., and Timms, J. F. (2002) *Mol. Cell. Proteomics* **1,** 91–98
31. Tonge, R., Shaw, J., Middleton, B., Rowlinson, R., Rayner, S., Young, J., Pognan, F., Hawkins, E., Currie, I., and Davison, M. (2001) *Proteomics* **1,** 377–396
32. Hayden, P. J., and Stevens, J. L. (1990) *Mol. Pharmacol.* **37,** 468–476
33. Aoudjit, L., Stanciu, M., Li, H., Lemay, S., and Takano, T. (2003) *Am. J. Physiol.* **285,** F765–F774
34. Zhan, Y., Cleveland, J. L., and Stevens, J. L. (1997) *Mol. Cell. Biol.* **17,** 6755–6764
35. Naaby-Hansen, S., Waterfield, M. D., and Cramer, R. (2001) *Trends Pharmacol. Sci.* **22,** 376–384
36. Cramer, R., Saxton, M., and Barnouin, K. (2004) in *Methods in Molecular Biology* (Fu, H., ed) Vol. 261, pp. 499–510, Humana Press, Totowa, NJ
37. Perkins, D. N., Pappin, D. J., Creasy, D. M., and Cottrell, J. S. (1999) *Electrophoresis* **20,** 3551–3567
38. Clauser, K. R., Baker, P., and Burlingame, A. L. (1999) *Anal. Chem.* **71,** 2871–2882
39. Benvenuti, S., Cramer, R., Quinn, C. C., Bruce, J., Zvelebil, M., Corless, S., Bond, J., Yang, A., Hockfield, S., Burlingame, A. L., Waterfield, M. D., and Jat, P. S. (2002) *Mol. Cell. Proteomics* **1,** 280–292
40. Schaeffer, V. H., and Stevens, J. L. (1987) *Mol. Pharmacol.* **32,** 293–298
41. Chen, Q., Yu, K., and Stevens, J. L. (1992) *J. Biol. Chem.* **267,** 24322–24327
42. Towndrow, K. M., Mertens, J. J., Jeong, J. K., Weber, T. J., Monks, T. J., and Lau, S. S. (2000) *Chem. Res. Toxicol.* **13,** 111–117
43. Landry, J., Lambert, H., Zhou, M., Lavoie, J. N., Hickey, E., Weber, L. A., and Anderson, C. W. (1992) *J. Biol. Chem.* **267,** 794–803
44. Oktay, M., Wary, K. K., Dans, M., Birge, R. B., and Giancotti, F. G. (1999) *J. Cell Biol.* **145,** 1461–1469
45. Ilic, D., Almeida, E. A., Schlaepfer, D. D., Dazin, P., Aizawa, S., and Damsky, C. H. (1998) *J. Cell Biol.* **143,** 547–560
46. Mehlen, P., Hickey, E., Weber, L. A., and Arrigo, A. P. (1997) *Biochem. Biophys. Res. Commun.* **241,** 187–192
47. Rogalla, T., Ehrnsperger, M., Preville, X., Kotlyarov, A., Lutsch, G., Ducasse, C., Paul, C., Wieske, M., Arrigo, A. P., Buchner, J., and Gaestel, M. (1999) *J. Biol. Chem.* **274,** 18947–18956
48. Lavoie, J. N., Lambert, H., Hickey, E., Weber, L. A., and Landry, J. (1995) *Mol. Cell. Biol.* **15,** 505–516
49. James, E. A., Gygi, S. P., Adams, M. L., Pierce, R. H., Fausto, N., Aebersold, R. H., Nelson, S. D., and Bruschi, S. A. (2002) *Biochemistry* **41,** 6789–6797
50. Mehlen, P., Kretz-Remy, C., Briolay, J., Fostan, P., Mirault, M. E., and Arrigo, A. P. (1995) *Biochem. J.* **312,** 367–375
51. Mehlen, P., Mehlen, A., Guillet, D., Preville, X., and Arrigo, A. P. (1995) *J. Cell. Biochem.* **58,** 248–259
52. Paul, C., Manero, F., Gonin, S., Kretz-Remy, C., Virot, S., and Arrigo, A. P. (2002) *Mol. Cell. Biol.* **22,** 816–834
53. Puthalakath, H., Villunger, A., O'Reilly, L. A., Beaumont, J. G., Coultas, L., Cheney, R. E., Huang, D. C., and Strasser, A. (2001) *Science* **293,** 1829–1832
54. Bruey, J. M., Ducasse, C., Bonniaud, P., Ravagnan, L., Susin, S. A., Diaz-Latoud, C., Gurbuxani, S., Arrigo, A. P., Kroemer, G., Solary, E., and Garrido, C. (2000) *Nat. Cell Biol.* **2,** 645–652

Heat Shock Protein 27 Is the Major Differentially Phosphorylated Protein Involved in Renal Epithelial Cellular Stress Response and Controls Focal Adhesion Organization and Apoptosis

Marjo de Graauw, Ine Tijdens, Rainer Cramer, Steve Corless, John F. Timms and Bob van de Water

J. Biol. Chem. 2005, 280:29885-29898.
doi: 10.1074/jbc.M412708200 originally published online June 8, 2005
